

State estimation for large-scale wastewater treatment plants^{*}

Jan Busch^{* 1} Peter Kühl^{** 2} Johannes P. Schlöder^{**}
Hans Georg Bock^{**} Wolfgang Marquardt^{*}

^{*} AVT Process Systems Engineering, RWTH Aachen University,
Germany

^{**} IWR, Heidelberg University, Germany

Abstract Many relevant process states in wastewater treatment are not measurable, or their measurements are subject to considerable uncertainty. This poses a serious problem for process monitoring and control. Model-based state estimation can provide estimates of the unknown states and increase the reliability of measurements. In this paper, an integrated approach is presented for the estimation problem employing unconventional, but technically feasible sensor networks. Using the ASM1 model in the reference scenario BSM1, the estimators EKF and MHE are evaluated. Very good estimation results for the system comprising of 78 states are found.

Keywords: state estimation, MHE, EKF, wastewater treatment, ASM, BSM1

1. INTRODUCTION

One of the key challenges in the operation of activated sludge wastewater treatment plants (WWTP) is the uncertainty about relevant process state values. E. g. the concentrations of active biomass and of soluble substrate are not measurable online, but they considerably influence process behavior. Some states such as the concentration of total suspended solids are measurable, but their measurements involve significant measurement errors. Reliable estimates of these states are of great value for different operational tasks such as process monitoring, online simulation, and advanced multi-variable control. They are a necessity for model-based control approaches based on dynamic process models (e. g. Busch et al., 2007). Model-based state estimation is one alternative to obtain such estimates. For a given process model, its success depends on the choice of a suitable hardware sensor network and of an appropriate estimation method.

The intention of this paper is to present sophisticated solutions to the state estimation problem for large-scale WWTP and to investigate two distinct state estimation approaches from the practitioner's point of view. First, an optimization-based approach determines the cheapest hardware sensor network that is required for the state estimation task. Second, Extended Kalman Filtering (EKF) and Moving Horizon Estimation (MHE) are employed to estimate the unknown model states of the large-scale WWTP model ASM1 employed in the BSM1 reference scenario (Copp, 2002). Large measurement errors, plant/model-mismatch, and unknown inflow concentrations are considered.

^{*} We thank the German research foundation (DFG) for the financial support in the project "Optimization-based process control of chemical processes" (grant MA 1188/27-1). Also BMBF grant 03BONCHD is gratefully acknowledged.

¹ present address: Bayer Technology Services, Leverkusen, Germany

² present address: BASF SE, Ludwigshafen, Germany

State estimation aims at statistically optimal estimates of measurable and unmeasurable process states. Dochain (2003) provides an overview of state and parameter estimation for chemical and biochemical processes focusing on small models. Lubenova et al. (2003) use an adaptive observer for a bioprocess models with 5 states. Goffaux and Vande Wouwer (2005) compare an asymptotic observer, an EKF, and a particle filter (PF) for a bioprocess model with 4 states. A model with approximately 40 states based on the ASM1 successor ASM3 is considered by Chai et al. (2007), who evaluate a KF, an EKF, and an unscented KF (UKF). No rigorous MHE implementation for WWTP has been reported.

Generally speaking, observers prove to be efficient for small-scale models with maybe up to 10 states. For larger models, observer design becomes challenging. An exception are asymptotic observers, which exhibit slow convergence of the estimates to the true values, but which do not require kinetic models. The EKF is the standard choice for large-scale models. It is easy to implement and much experience is available concerning its design and tuning. It is not clear whether the related UKF and PF can significantly outperform the EKF in practical implementations. The MHE is a promising option, but it is not clear whether its increased implementation effort is justified by better estimation results in WWTP applications. Large-scale simulation case studies are rare, and real-life case studies are not available. Also, while the properties of the hardware sensor network are decisive for the success of any state estimation approach, this aspect has not been treated much with respect to WWTP applications.

Ideally, the choice of a sensor network, of a process model, and of the estimator should be considered as an integrated problem. This is beyond our possibilities today. The sensor networks used in this study are obtained by a simple optimization-based sensor network design approach. An observable system for a given large-scale plant model

involving 78 differential states is obtained. An EKF and an MHE are then employed as state estimators.

2. PROCESS AND PROCESS MODEL

The simulation study is based on the BSM1 (Copp, 2002), which has been developed as a benchmark scenario for the evaluation and comparison of different control approaches for WWTP. The plant layout is depicted in Fig. 1. Q_i and \mathbf{Z}_i refer to the flow rate and vector of concentrations for stream i . The inflow is mixed with two recycle streams before entering the plant. Two denitrification basins (each 1000 m³) are followed by three aerated nitrification basins (each 1333 m³). The first recycle a is withdrawn from the last nitrification basin. The settler used in the BSM1 is replaced by a membrane filtration unit, which is located in a separate 250 m³ basin and which is modeled as an ideal splitter. The product stream e as well as a second recycle r and a waste stream w leave the membrane basin. All basins are assumed to be well-mixed.

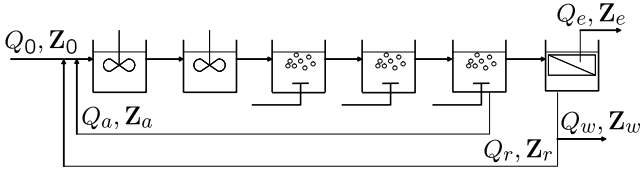


Figure 1. Modified BSM1 plant layout.

The degradation processes in the five biological basins are described by the ASM1 (Henze et al., 1987) with parameters taken from Copp (2002). The ASM1 describes 8 reactions and the component concentrations of inert soluble matter S_I , soluble substrate S_S , inert particulate matter X_I , particulate substrate X_S , heterotrophic biomass $X_{B,H}$, autotrophic biomass $X_{B,A}$, particulate inert metabolism products X_P , dissolved oxygen (DO) S_O , nitrate S_{NO} , ammonia S_{NH} , soluble organic nitrogen S_{ND} , particulate organic nitrogen X_{ND} , and the alkalinity S_{ALK} . The resulting model comprising mass balances and the kinetic model contains 78 differential states. It is formulated as a semi-explicit differential-algebraic model according to

$$\dot{\mathbf{x}} = \mathbf{f}(\mathbf{x}, \mathbf{z}, \mathbf{u}, \mathbf{p}), \quad (1)$$

$$0 = \mathbf{g}(\mathbf{x}, \mathbf{z}, \mathbf{u}, \mathbf{p}), \quad (2)$$

$$\mathbf{y} = \mathbf{M} \cdot \mathbf{x}. \quad (3)$$

\mathbf{x} are differential and \mathbf{z} are algebraic states, \mathbf{u} are the manipulated variables, and \mathbf{p} are the parameters. \mathbf{y} are the measurable outputs and \mathbf{M} is the measurement matrix. Note that for the BSM1 scenario, $\mathbf{g}(\cdot)$ represents defining equations that can explicitly be solved for \mathbf{z} . Generally $\mathbf{g}(\cdot)$ suffices to be of index 1.

The BSM1 benchmark describes a dry weather scenario for a period of 100 days with constant manipulated variables, inflow rates, and inflow concentrations to reach a steady state. This is followed by a period of 14 days with dynamic inflow conditions. One of the three different dynamic scenarios, the *storm scenario*, is used in this paper. It is characterized by dry weather inflow superposed by storm events on days 9 and 11. Exemplarily, the corresponding inflow rate and ammonia inflow concentration are depicted in Fig. 2.

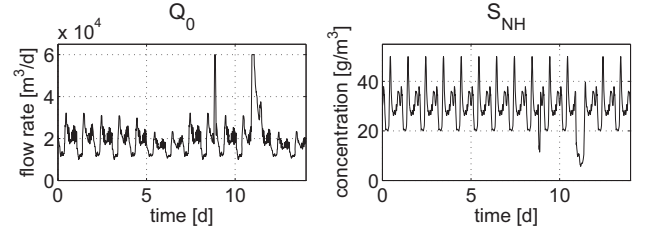


Figure 2. Inflow rate Q_0 and ammonia inflow concentration $Z_{0,S_{NH}}$.

3. SENSOR NETWORK DESIGN

The success of a state estimation approach depends on the process model, on the state estimation algorithm, and on the sensor network which supplies the measurements. Optimal sensor network design aims at the sensor network which leads to optimal state estimates at limited cost, or similarly, reliable state estimates at minimum cost (Singh and Hahn, 2005). So far, systematic approaches to this important aspect of state estimation have been neglected in the literature on WWTP applications. Rather, the sensor network is chosen based on experience and intuition.

The approach to obtain the sensor networks as used in this study is outlined in the following, details are presented in Busch et al. (2009). A sensor network is fully defined by the measurement matrix \mathbf{M} (Eq. (3)), which relates process states \mathbf{x} to measurements \mathbf{y} . By assigning prices to the measurement hardware, a cost function $\phi = \phi(\mathbf{M})$ is obtained, which describes the cost of the sensor network. The relevant constraint for the sensor network is that it needs to yield an observable system. Hence, the non-linear process model is linearized at many instances along a typical process trajectory, and observability is checked for each of these instances by a suitable criterium. Finally, a genetic optimization algorithm is employed to find the sensor network with the minimum cost $\phi(\mathbf{M})$ which still fulfills the observability constraints (Heyen and Gerken, 2002). The approach is applied to the simulation scenario described in Section 2. Considering 8 technically feasible measurements in 6 basins gives a total of $2^{6 \cdot 8} \approx 2.8 \cdot 10^{14}$ measurement configurations.

The following sensor network is found to give observability at minimum cost: $COD_{1,1}, S_{ALK,1}, S_{O,2}, X_{TS,5}$, where the numeric index refers to the basin number. COD is the chemical oxygen demand. This result is quite surprising, as it implies that only four hardware sensors suffice to estimate all 78 model states. Some standard hardware sensors, which are commonly available at WWTP, are added to the sensor network. These are DO sensors in the aerated basins as well as nitrate, ammonia, alkalinity, and COD measurements in the effluent.

4. STATE ESTIMATORS

State estimation refers to retrieving all states of a dynamic system in real-time by utilizing available measurements, possibly in combination with a process model. While the state estimation problem is largely solved for *linear systems*, e.g., by the Kalman Filter, the problem becomes significantly more difficult for non-linear systems. Most methods are extensions of linear state estimators, such

as the extended Kalman Filter (EKF), described e. g. in Becerra et al. (2001). A *non-linear* version of MHE is presented in Rao et al. (2003). A comparison of EKF and non-linear MHE applied to the BSM1 scenario is presented in Section 5. In the following, main principles and implementation details are reviewed.

4.1 Extended Kalman Filter

The Kalman Filter is a recursive method for state estimation. It consists of a prediction step (time update) and a measurement update. Past data is summarized and carried on by means of suitable statistics. For a non-linear system in discrete-time with measurement noise $\mathbf{v}_k \sim \mathcal{N}(0, \tilde{\mathbf{V}})$ and process noise $\boldsymbol{\mu}_k \sim \mathcal{N}(0, \tilde{\mathbf{W}})$

$$\mathbf{x}_k = \mathbf{f}_k(\mathbf{x}_{k-1}, \mathbf{z}_{k-1}, \mathbf{u}_{k-1}, \mathbf{p}_{k-1}) + \boldsymbol{\mu}_k, \quad (4)$$

$$\mathbf{0} = \mathbf{g}_k(\mathbf{x}_{k-1}, \mathbf{z}_{k-1}, \mathbf{u}_{k-1}, \mathbf{p}_{k-1}), \quad (5)$$

$$\mathbf{y}_k = \mathbf{M} \cdot \mathbf{x}_k + \mathbf{v}_k, \quad (6)$$

where k denotes the sampling instant, the respective filter equations in their most common form are:

Time update:

$$\hat{\mathbf{x}}_k^- = \mathbf{f}_k(\hat{\mathbf{x}}_{k-1}^-, \mathbf{z}_{k-1}, \mathbf{u}_{k-1}, \mathbf{p}_{k-1}), \quad (7a)$$

$$\mathbf{P}_k^- = \frac{\partial \mathbf{f}_k}{\partial \mathbf{x}_{k-1}} \bigg|_{\hat{\mathbf{x}}_{k-1}^-} \cdot \mathbf{P}_{k-1} \cdot \frac{\partial \mathbf{f}_k}{\partial \mathbf{x}_{k-1}} \bigg|_{\hat{\mathbf{x}}_{k-1}^-}^T + \mathbf{W}, \quad (7b)$$

Measurement update:

$$\mathbf{K}_k = \mathbf{P}_k^- \cdot \mathbf{M}_d^T \cdot (\mathbf{M}_d \cdot \mathbf{P}_k^- \cdot \mathbf{M}_d^T + \mathbf{V})^{-1}, \quad (8a)$$

$$\mathbf{P}_k = (\mathbb{I} - \mathbf{K}_k \cdot \mathbf{M}_d) \cdot \mathbf{P}_k^-, \quad (8b)$$

$$\hat{\mathbf{x}}_k = \hat{\mathbf{x}}_k^- + \mathbf{K}_k \cdot (\mathbf{y}_k - \mathbf{M}_d \cdot \hat{\mathbf{x}}_k^-), \quad (8c)$$

$$\mathbf{0} = \mathbf{g}_k(\hat{\mathbf{x}}_k, \mathbf{z}_k, \mathbf{u}_k, \mathbf{p}_k). \quad (8d)$$

\mathbf{f}_k typically represents a numerical integration of the continuous system Eq. (1) from time t_{k-1} to t_k with initial values \mathbf{x}_{k-1} . The matrix \mathbf{P}_k is the covariance matrix associated with the state estimates $\hat{\mathbf{x}}_k$ at sampling time k . It reflects the confidence one can have in this estimate. The matrices \mathbf{V} and \mathbf{W} describe the assumed covariances of measurement noise and process noise, respectively. The Kalman Filter gain \mathbf{K}_k then reflects the trade-off between the measurements and the process model.

4.2 Moving Horizon Estimation

A drawback of most estimation methods is that they cannot deal with known constraints on the estimated states. In the MHE scheme, such constraints are naturally incorporated in the optimization problem. The formulation also allows to additionally estimate process parameters without reformulating them as dummy states.

Unlike the EKF, the MHE uses more than just the most recent measurements: At a certain time t_j a number of $M+1$ measurements ($\mathbf{y}_{j-M}, \dots, \mathbf{y}_j$) associated with past time instants $t_{j-M} < \dots < t_j$ are explicitly used for estimation. The length L of the time horizon $[t_j, \dots, t_{j-M}]$ is defined as $L := j - M$. It is assumed that measurement and process noise are normally distributed with zero mean and covariance matrices \mathbf{V} and \mathbf{W} . Additionally, a Gaussian distribution is assumed for $\mathbf{x}(t_L)$ and \mathbf{p} at the beginning of the horizon, with expectation value $(\bar{\mathbf{x}}_L, \bar{\mathbf{p}}_L)$ and a block-diagonal covariance matrix $\boldsymbol{\Pi}_L$ with block elements $\boldsymbol{\Pi}_{\bar{\mathbf{x}}, L}$ and $\boldsymbol{\Pi}_{\bar{\mathbf{p}}, L}$.

The state estimation problem to be solved at time t_k – given the measurements \mathbf{y}_j for $j = L, L+1, \dots, k$, the known input $\mathbf{u}(t)$ for $t \in [t_L, t_k]$ and given $(\bar{\mathbf{x}}_L, \bar{\mathbf{p}}_L)$ and $\boldsymbol{\Pi}_L$ – has the following form:

$$\min_{\mathbf{x}(\cdot), \mathbf{p}} \left(\|\mathbf{x}(t_L) - \bar{\mathbf{x}}_L\|_{\boldsymbol{\Pi}_{\bar{\mathbf{x}}, L}}^2 + \|\mathbf{p} - \bar{\mathbf{p}}_L\|_{\boldsymbol{\Pi}_{\bar{\mathbf{p}}, L}}^2 + \sum_{j=L}^k \|\mathbf{y}_j - \mathbf{M} \cdot \mathbf{x}(t_j)\|_{\mathbf{V}}^2 \right) \quad (9)$$

$$\text{s.t. } \dot{\mathbf{x}}(t) = \mathbf{f}(\mathbf{x}(t), \mathbf{z}(t), \mathbf{u}(t), \mathbf{p}), \quad t \in [t_L, t_k], \quad (10a)$$

$$\mathbf{0} = \mathbf{g}(\mathbf{x}(t), \mathbf{z}(t), \mathbf{u}(t), \mathbf{p}), \quad (10b)$$

$$\mathbf{x}_{\min} \leq \mathbf{x}(t) \leq \mathbf{x}_{\max}, \quad (10c)$$

$$\mathbf{p}_{\min} \leq \mathbf{p} \leq \mathbf{p}_{\max}, \quad (10d)$$

where the applied norm is defined as $\|\mathbf{x}\|_{\mathbf{V}}^2 := \mathbf{x}^T \mathbf{V}^{-1} \mathbf{x}$.

At each new sampling time t_k , one new measurement vector \mathbf{y}_k enters the set of measurements, while the last one \mathbf{y}_L becomes \mathbf{y}_{L-1} and drops out of the horizon.

The initial weight terms $\|\mathbf{x}(t_L) - \bar{\mathbf{x}}_L\|_{\boldsymbol{\Pi}_{\bar{\mathbf{x}}, L}}^2$ and $\|\mathbf{p} - \bar{\mathbf{p}}_L\|_{\boldsymbol{\Pi}_{\bar{\mathbf{p}}, L}}^2$ (often called "arrival costs") summarize information in the MHE problem prior to the horizon beginning at time t_L and also reflect a cumulated effect of process noise on the process. A typical approach is to compute the arrival costs by Kalman Filter updates of $\bar{\mathbf{x}}_L$ and $\bar{\mathbf{p}}_L$. As for the optimal length of the estimation horizon, no general results are available, yet. Horizon length and the weighting matrices \mathbf{V}^{-1} , $\boldsymbol{\Pi}^{-1}$ are the tuning parameters. Note that an extended MHE formulation exists that explicitly incorporates process noise (Rao et al., 2003; Diehl et al., 2006).

A necessity for the MHE scheme to work is a fast and reliable numerical scheme for the constrained non-linear dynamic optimization problem (9). The implementation in this work makes use of MUSCOD-II (Leineweber et al., 2003), which is based on a direct multiple shooting approach, see, e. g. , (Bock et al., 2007). For real-time feasibility, the least-squares problem at each time instant t_k is not solved to convergence. Instead, only one Gauss-Newton iteration is performed, combined with a meaningful shift of the problem variables. More information on this so-called *real-time iteration approach* along with other implementation details can be found in Diehl et al. (2006).

5. CASE STUDY

EKF and MHE are applied to the process model and scenario described in Section 2 and the sensor network calculated in Section 3. The estimation task was made increasingly difficult to evaluate the estimation performance under nominal and more realistic conditions.

Only little effort has been devoted to the fine-tuning of the estimators. This is intentional, since the aim of the study is to investigate the practical applicability and general performance of the two estimation methods. The tuning matrices \mathbf{W} and \mathbf{V} for the EKF and the MHE reflect covariances based on an assumed standard deviation of 5% of the initial values \mathbf{x}_0 and "initial measurements" $\mathbf{M} \cdot \mathbf{x}_0$. The MHE uses an estimation horizon of 5 measurement samples.

The initial guess for $\hat{\mathbf{x}}_0$ is deliberately set to $1.3 \cdot \mathbf{x}_0$ to introduce a strong initial offset. The measurements are corrupted by white noise \mathbf{v} with a standard deviation of 5% of the initial measurements: $\mathbf{y}_k = \mathbf{M} \cdot \mathbf{x}_k + \mathbf{v}_k$. The sampling interval is set to 15 minutes. In the following, the quality of the estimation results will be illustrated by the estimates of the third basin, which is the one with the least measurements (only DO concentration). The DO concentration is not visualized as the estimates always closely follow the true values.

5.1 Nominal process

In the first scenario, no process noise is added and perfect knowledge of the inflow rate and concentrations is assumed. The estimated state values quickly converge from their initial offset to the true values (not shown). Only the concentration of X_P shows some occasional offset. The root of the cumulated squared relative error (RCSE) averaged over all J samplings is used in the following as a measure to compare the overall estimation performance:

$$\text{RCSE} = \frac{1}{J} \sum_{k=1}^J \sqrt{\sum_{i=1}^N \left(\frac{\hat{x}_{i,k} - x_{i,k}}{x_{i,k}} \right)^2}, \quad (11)$$

where J is the number of samples $x_{i,k}$ and $\hat{x}_{i,k}$ and N is the number of states. The RCSE values for the different simulation case studies are stated in Table 1. For the EKF and the MHE with known inputs and no process noise, RCSE of 0.3 and 0.4 are obtained, respectively.

Table 1. RCSE for the estimated states of different simulation scenarios and estimators.

Estimator	Known inputs, no process noise	Known inputs, process noise	Unknown inputs, process noise
EKF	0.3	0.7	1.8
MHE	0.4	0.8	1.6

5.2 Process noise

Process noise is added to introduce plant/model-mismatch to the problem. The process noise $\boldsymbol{\mu}$ has zero mean and a standard deviation of 5% of the initial states and enters the discrete time simulation model according to

$$\mathbf{x}_{k+1} = \mathbf{f}(\mathbf{x}_k, \mathbf{z}_k, \mathbf{u}_k, \mathbf{p}_k) + \boldsymbol{\mu}_k, \quad (12a)$$

$$\mathbf{0} = \mathbf{g}(\mathbf{x}_k, \mathbf{z}_k, \mathbf{u}_k, \mathbf{p}_k). \quad (12b)$$

Noise-induced negative states representing concentrations are set to zero to ensure that the equations remain physically feasible. The estimation results are similar for the EKF and the MHE. Exemplarily, Fig. 3 shows the results for the third basin using the MHE. Deviations from the true trajectories are observed, but the estimation result averaged over all samples remains satisfactory for both estimators. The RCSE of the EKF and the MHE changes from 0.3 to 0.7 and from 0.4 to 0.8, respectively (Table 1). This result is not surprising, as the process noise now deviates the measured outputs, complicated even further by the process nonlinearities which are not fully captured by the estimators.

5.3 Unknown inflow concentrations

Up to now it has been assumed that the inflow rate and concentrations are perfectly known. This assumption is

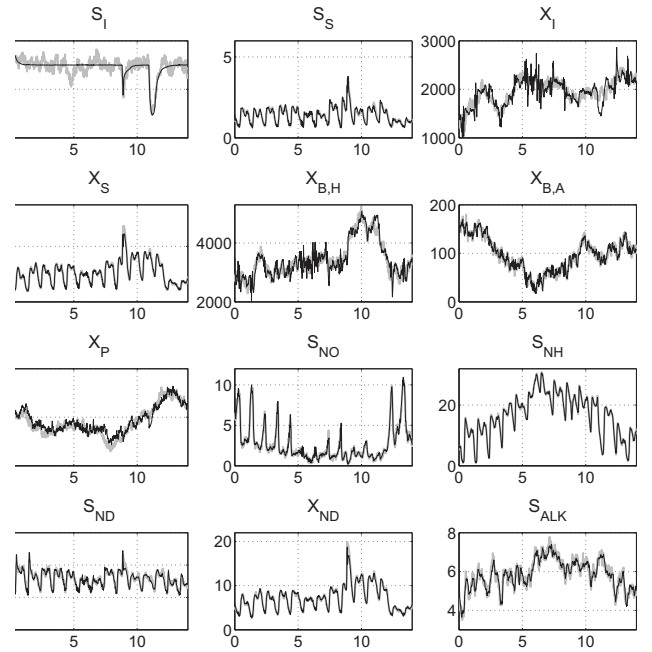


Figure 3. MHE with 5% process noise, third basin. The x-axis shows the time in days, and the y-axis shows the concentrations in $[\text{g}/\text{m}^3]$. The alkalinity S_{ALK} is dimensionless. The graphs show the true process state values (light grey) and the estimates (black).

not realistic. While the inflow rate is indeed well-known, at least part of the inflow concentrations are not. Typically historic data is employed to obtain daily, weekly, and yearly trends and patterns of e.g. the concentrations or the composition of the COD. However, a substantial bias between these predictions and the real inflow concentrations must be expected. A worst case situation is considered in the following: The inflow concentrations of soluble inert matter S_I , soluble substrate S_S , particulate inert matter X_I , particulate substrate X_S , heterotrophic biomass $X_{B,H}$, as well as soluble S_{ND} and particulate organic nitrogen X_{ND} are treated as unknown model inputs. The inflow concentrations of DO S_O , autotrophic biomass $X_{B,A}$, metabolism products X_P , and nitrate X_{NH} are set to zero, and the alkalinity S_{ALK} is set to 7, which corresponds to typical inflow characteristics as well as to the BSM1. The inflow rate Q_0 and the inflow ammonia concentration S_{NH} are measurable. The unknown inputs need to be estimated together with the unknown states.

First, a new sensor network is determined by applying the optimization procedure outlined in Section 3 to an extended model, which considers the unknown inflow concentrations as additional model states (Busch et al., 2009). The resulting sensor network is more complex than the network used for the estimation of the nominal process, but still technically and economically feasible:

$$X_{TS,1}, S_{ALK,1}, BOD_2, BOD_3, S_{O,3}, S_{ALK,3}, \\ S_{ALK,4}, COD_5, COD_6,$$

where BOD is the biological oxygen demand. The same standard measurements as discussed in Section 3 are added to the sensor network.

The estimation of the model parameters such as input concentrations is an integrated part of the MHE implementation and thus can be pursued very easily (see Section 4). For the EKF, the effort is slightly higher. Here, to additionally estimate process parameters, these have to be formulated as additional differential states \mathbf{x}_p obeying the trivial differential equation $\dot{\mathbf{x}}_p = \mathbf{0}$ with initial values $\mathbf{x}_p(0) = \mathbf{p}$. The EKF then estimates the augmented state vector $(\mathbf{x}^T \mathbf{x}_p^T)^T$. Note that the covariance matrix \mathbf{W} has to be adapted to the new state vector. The expected process noise standard deviation of the unknown parameters is specified as 5% of their nominal values. The initial guess for the inflow concentrations is also disturbed by +30%. Fig. 4 depicts the estimated states for the third basin. The estimation performance is again satisfactorily except for two states. The estimation of inert particulate matter X_I shows considerable offset from the true values. This is, however, not severe, as inert matter does not affect the reaction kinetics and is hence irrelevant for process prediction. The second state to exhibit a significant offset is the concentration of heterotrophic biomass $X_{B,H}$. This is more serious as heterotrophic biomass is responsible for the degradation of substrate and nitrate. Whether the offset is critical, e.g. in model-based control approaches, needs to be evaluated in future research. Fine-tuning of the estimator might further minimize the deviation. The overall RCSE is 1.8 for the states (Table 1) and 2.0 for the parameters.

Fig. 5 shows the estimation results for the states in the third basin as obtained by the MHE. The results do not differ much from those of the EKF. Again, the two states inert particulate matter X_I and heterotrophic biomass $X_{B,H}$ show the largest deviations. From visual inspection, the first seems to stay closer to the true value but then exhibits a sudden and sharp drop which is not present in the real trend. The overall RCSE for this case is 1.6 (Table 1) and hence slightly better than for the EKF. The estimated parameters achieve an RCSE of 2.1.

The estimated inflow concentrations are depicted exemplarily for the EKF in Fig. 6. All estimates exhibit high-frequency oscillations, which could probably also be improved by fine-tuning of the estimators. The estimation of the concentration of heterotrophic biomass $X_{B,H}$ again shows a stronger offset during days 11 to 13 following the second storm event but returns to the true value eventually. The graphs of inert particulate matter X_I and particulate organic nitrogen X_{ND} show that the estimates are not able to follow sudden concentration peaks (day 9).

The main trends in the inflow data are captured well, but it is not clear especially with respect to the concentrations of inert particulate matter X_I and heterotrophic biomass $X_{B,H}$ whether these parameter are actually observable. To clarify the issue, additional scenarios have been calculated which show that the parameters are indeed observable, but that their influence on the noisy process and process measurements is small, so that it is not possible to resolve higher frequent variations Busch et al. (2009).

5.4 Computation times

A general belief that can often be found is that optimization-based estimation methods such as MHE are impractical

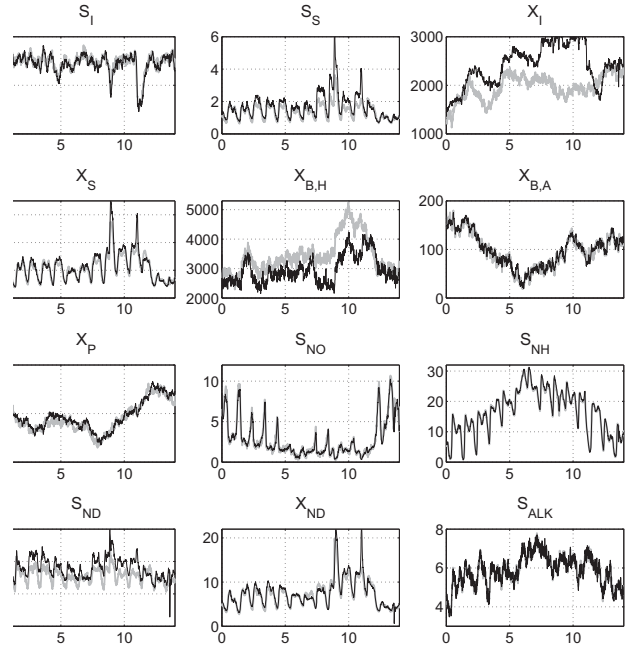


Figure 4. EKF with unknown inflow concentrations and 5% process noise, third basin. The x-axis shows the time in days, and the y-axis shows the concentrations in $[\text{g}/\text{m}^3]$. The alkalinity S_{ALK} is dimensionless. The graphs show the true process state values (light grey) and the estimates (black).

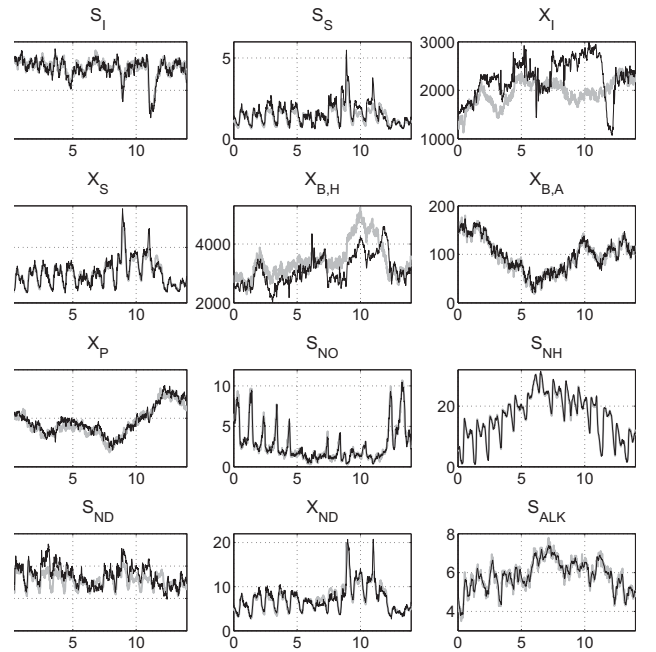


Figure 5. MHE with unknown inflow concentrations and 5% process noise, third basin. The x-axis shows the time in days, and the y-axis shows the concentrations in $[\text{g}/\text{m}^3]$. The alkalinity S_{ALK} is dimensionless. The graphs show the true process state values (light grey) and the estimates (black).

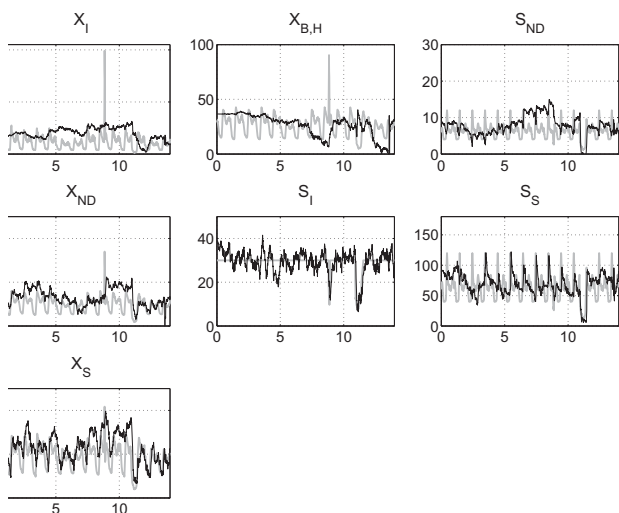


Figure 6. EKF with unknown inflow concentrations and 5% process noise. The x-axis shows the time in days, and the y-axis shows the inflow concentrations in $[g/m^3]$. The graphs show the true process state values (light grey) and the estimates (black).

because of the excessive computation times to be expected. Indeed the time required to solve a constrained optimization problem to full convergence will necessarily be larger than recursively solving the corresponding unconstrained problem. However, the numerical approach sketched in Section 4 can significantly reduce the computation times. In the case studies described, the average computation time for the MHE was in the range of a few seconds with a maximum lower than 10 seconds on a Pentium 4 machine with 2.8 GHz, 1024 kB L2 cache, 1 GB RAM under Suse Linux 9.3. This is by far fast enough for the estimation tasks for WWTP.

6. CONCLUSIONS

In this paper inflow and state estimation approaches for large-scale wastewater treatment plants are presented. The process is based on the reference scenario BSM1 and employs the dynamic, non-linear process model ASM1. The two prominent state estimators EKF and MHE are evaluated. Large process and measurement disturbances as well as unknown influent conditions have been considered.

The results show that it is possible to yield a fully observable system with an unconventional sensor network of moderate complexity. Both the EKF and the MHE show good estimation performance even in difficult conditions. The EKF shows a marginally better performance for the scenarios with known inflow concentrations. For unknown inflow concentrations, the MHE delivers slightly better state estimates. These do not fully justify the higher implementational effort for the MHE. However, its simple and straightforward handling of unknown inflow conditions and parameters is an advantage over the EKF. The computation times presented here show that the EKF as well as the MHE are real-time feasible for WWTP.

REFERENCES

- Becerra, V.M., Roberts, P.D., and Griffiths, G.W. (2001). Applying the extended Kalman Filter to systems described by nonlinear differential-algebraic equations. *Control Eng. Pract.*, 9, 267–281.
- Bock, H., Kostina, E., and Schlöder, J.P. (2007). Numerical methods for parameter estimation in nonlinear daes. *GAMM Mitteilungen*, 30/2, 352–375.
- Busch, J., Kuehl, P., Gerkens, C., Marquardt, W., Schlöder, J.P., and Bock, H.G. (2009). State estimation for large-scale wastewater treatment plants. *Wat. Res.* (in preparation).
- Busch, J., Oldenburg, J., Santos, M., Cruse, A., and Marquardt, W. (2007). Dynamic predictive scheduling of operational strategies for continuous processes using mixed-logic dynamic optimization. *Comput. Chem. Eng.*, 31(5–6), 574–587.
- Chai, Q., Furenes, B., and Lie, B. (2007). Comparison of state estimation techniques, applied to a biological wastewater treatment process. In *Proceedings of the 10th IFAC Symposium on Computer Applications in Biotechnology*, 353–358. Cancun, Mexico.
- Copp, J.B. (ed.) (2002). *The COST Simulation Benchmark. Description and Simulator Manual*. Office for Official Publications of the European Communities, Luxembourg.
- Diehl, M., Kuehl, P., Bock, H.G., and Schlöder, J.P. (2006). Schnelle Algorithmen für die Zustands- und Parameterschätzung auf bewegten Horizonten. *Automatisierungstechnik*, 54(12), 602–613.
- Dochain, D. (2003). State and parameter estimation in chemical and biochemical processes: a tutorial. *J. Process Contr.*, 13, 801–818.
- Goffaux, G. and Vande Wouwer, A. (2005). Bioprocess state estimation: Some classical and less classical approaches. In T.M. et al. (ed.), *Control and Observer Design*, 111–128. Springer, Berlin, Heidelberg.
- Henze, M., Grady Jr., C.P.L., Gujer, W., Marais, G.V.R., and Matsuo, T. (1987). A general model for single-sludge wastewater treatment systems. *Water Res.*, 21(5), 505–515.
- Heyen, G. and Gerkens, C. (2002). Application d’algorithmes génétiques à la synthèse de systèmes de mesure redondants. In *Proceedings of SIMO 2002 Congress*. Toulouse, France.
- Leineweber, D.B., Schäfer, A., Bock, H.G., and Schlöder, J.P. (2003). An efficient multiple shooting based reduced SQP strategy for large-scale dynamic process optimization. Part II: Software aspects and applications. *Comput. Chem. Eng.*, 27, 167–174.
- Lubenova, V., Rocha, I., and Ferreira, E.C. (2003). Estimation of multiple biomass growth rates and biomass concentration in a class of bioprocesses. *Bioproc. Biosyst. Eng.*, 25, 395–406.
- Rao, C.V., Rawlings, J.B., and Mayne, D.Q. (2003). Constrained state estimation for nonlinear discrete-time systems: Stability and moving horizon approximations. *IEEE T. Automat. Contr.*, 48(2), 246–258.
- Singh, A.K. and Hahn, J. (2005). Determining optimal sensor locations for state and parameter estimation for stable nonlinear systems. *Ind. Eng. Chem. Res.*, 44(15), 5645–5659.